Hindawi
Advances in Materials Science and Engineering
Volume 2022, Article ID 7210265, 14 pages
https://doi.org/10.1155/2022/7210265

Research Article

Parameter Optimization and Machining Performance of Inconel 625 with Nanoparticles Dispersed in Biolubricant

T. Mohanraj,[1] **N. Radhika**,[1] **S. Aswin Nanda**,[1] **V. Vignesh**,[1] **B. Jayaraman**,[1] **K. R. Ratana Selvan**,[1] **and Yesgat Admassu**[2]

[1]*Department of Mechanical Engineering, Amrita School of Engineering, Amrita Vishwa Vidyapeetham, Coimbatore, India*
[2]*Institute of Research Development, Defence University College of Engineering, Bishoftu, Ethiopia*

Correspondence should be addressed to Yesgat Admassu; yesgat.admassu@dec.edu.et

Received 17 June 2022; Accepted 20 July 2022; Published 24 August 2022

Academic Editor: Pudhupalayam Muthukutti Gopal

Productivity and cost-effectiveness are essential components of any long-term manufacturing system. While quantity and quality are linked to productivity, the economy focuses on energy-efficient processes that produce a high output-to-input ratio. Hard-to-cut materials have always been difficult to machine because of more significant tool wear and power losses. Inconel 625 is a hard material used in aerospace and underwater applications and is milled using biolubricants with nanoparticles. Palm oil is considered a biolubricant, and titanium dioxide (TiO_2) and copper oxide (CuO) are selected as nanoparticles. When the combination of biolubricants and nanoparticles is added to the workpiece's surface, it enhanced some properties while machining. Experiments involving four factors with four levels were carried out using the Taguchi design of experiments (DoE). The feed, depth of cut, speed, and coolant with nanoparticle additives were all factors. The responses were surface roughness, spindle vibration along *X*, *Y*, and *Z* axes, and material removal rate. Technique for Order of Preference by Similarity to Ideal Solution (TOPSIS) was used to alter the multiresponse optimization problem to a single-response optimization problem. The S/N of TOPSIS closeness coefficients was calculated, and the optimal machining conditions were determined. Surface roughness, material removal rate, and spindle vibration were reduced by 3.10%, 6.14%, 7.54% (*Vx*), and 6.78% (*Vz*), respectively, due to the TOPSIS optimization.

1. Introduction

Inconel 625's enhanced mechanical properties, outstanding weldability, and high oxidation and corrosion resistance, nickel-based aerospace alloys have gained popularity. Inconel 625 is widely used in manufacturing, especially for aircraft structures, springs, turbine blades, submarine bellows, steam power plants, and oceanographic devices [1]. Due to its meager thermal conductivity, the formation of built-up edges, and a greater sticking or welding propensity to cutting edges, Inconel 625's machinability is considered poor [2] and classified as a difficult-to-machine material. Furthermore, due to Inconel 625's low heat transfer rate, a large portion of the cutting energy is converted into heat during machining, which remains in the tool-workpiece interface for a longer time. High localized temperatures in the machining region result from heat generation, causing tool material softening and rapid tool wear, decreasing tool life, and compromising machined surface integrity. The use of cutting fluids is required to solve these issues. Most traditional machining fluids contain hazardous chemical constituents that can pollute the environment, cause biological problems for workers, contaminate soil, and pollute water during disposal [3, 4]. Furthermore, cutting fluids account for roughly 17% of machining costs, while tooling costs account for only 8% [5, 6]. Many attempts have been made to reduce cutting fluids to make material removal processes more environmentally friendly [7]. The growing interest in tracking all elements of the material removal process has resulted from the metal-based industry's main challenge of increasing the quality and productivity of machined parts [8].

Dry cutting, or machining without the need for any cutting fluid, is one of the best machining options for achieving green manufacturing. However, when dry-machining Inconel, the work material bonds firmly to the tool surface, resulting in early tool failure and poor surface quality. Furthermore, Inconel's high mechanical strength and poor thermal conductivity result in unfavorable residual stresses, surface irregularities, and burning/overheating in the cutting zone when machining without coolant [9]. The surface roughness of the machined product can affect various areas of its operation, including gentle friction, heat generation, the ability to distribute and hold a lubricant, wear, and a material's ability to withstand fatigue [10]. Dry cutting also necessitates using unique cutting tool materials such as ceramic, PCD, PCBN, and careful tool geometry and specific coatings. Therefore, to facilitate heat transfer from the tool–chip interface, these tacky alloys are typically machined under wet cutting conditions, which results in high manufacturing costs, worker health risks, and severe environmental problems [11]. Due to the specific inherent properties and their capacity to biodegrade, vegetable oils are seen as alternatives to mineral oils in lubricant formulations.

Vegetable oils have a high flash point, viscosity index, lubricity, and lower evaporative loss than mineral oils [12]. Plant oils are extracted by applying pressure to the pertinent part of a plant and squeezing the oil out [13]. Plant oils (edible and nonedible) can also be extracted by dissolving plant parts in water, distilling the oil, or infusing plant parts with a base oil. Various studies have demonstrated the value of edible vegetable oils such as coconut oil [14], palm oil [15], soya bean oil [16], and canola oil [17] as an environmentally friendly lubricant for machining. The novelty was premised on the fact that using cooling/lubrication circumstances and depth of cut as input variables improved the manufacturing system's sustainability and efficiency. This study is based on the idea that productivity results from quality, utilization, and efficiency working together.

The utilization of nanoparticles in various base fluids has received a lot of interest in the last decade [18]. The nanoparticles dispersed in water, for instance, can improve the thermal conductivity, and it is a suitable heat transfer fluid, especially for solar collectors [19]. Nano coolants (the dispersal of nanoparticles in water or ethylene glycol) have been studied for real-world problems since the early 2000s [20]. Nanoparticles added to the lubricant are thought to provide antifriction and antiwear properties. On the other hand, the improved characteristics are entirely determined by nanoparticle characteristics like shape, size, and concentration. Moreover, it has been reported that adding a suitable amount of nanoparticles to lubricating oil improves antifriction and antiwear characteristics [21]. These terms cover the manufacturing process, including surface roughness, material removal rate, and spindle vibration. These responses are optimized by combining constructive process parameters like feed speed and cutting depth. Taguchi design of experiment (DoE) is used to optimize the input parameters collectively, as they would alternatively behave differently in different responses. The goal is to optimize the input parameters based on the responses that are both sustainable and constructive at the same time.

Table 1: Properties of palm oil.

Oils	Color	Density (g/cm^3)	Dynamic viscosity (mPa·s)
Palm oil	Light yellow	0.89	77.19

Taguchi's DoE is an excellent tool for optimization because it is simple and efficient. Taguchi assists in selecting a control variable combination that significantly reduces the impact of noise. Minimizing tool costs is necessary to be cost-effective in manufacturing [22]. Variations recommended that machining irregularity could be reduced if appropriate values and requirements were used [23]. Technique for Order of Preference by Similarity to Ideal Solution (TOPSIS) selects the alternative closest to the ideal solution and farthest from the ideal negative alternative. It is helpful in cases where there are a lot of requirements and substitutes [24]. It is based on the theory of an optimum moving solution from which it tries to negotiate the result that is the closest. The smallest distance from the positive ideal solution (PIS) and the greatest distance from the negative ideal solution (NIS) are used to rank the options. TOPSIS explores the ranges of both PIS and NIS, ranking candidates based on their relative proximity and combining the two distance measurements [25]. Taguchi's DoE was combined with the TOPSIS to identify the processing parameters for milling the Inconel 625 alloy. Surface roughness, spindle vibration, and MRR were all taken into account. They discovered that, after optimization, machining performance improved [26]. The novelty of this research lies in the combination of biolubricants and nanoparticles that are used. Inconel 625 has not been machined with the current choice of biolubricants and nanoparticles. The responses such as surface roughness (Ra), material removal rate (MRR), and vibration have not been recorded for this particular combination.

2. Materials and Method

2.1. Oils and Nanoparticles. After carefully considering the literature review and availability of the materials, palm oil has been chosen. The nanoparticles chosen are TiO_2 and CuO. The nanoparticles are biocompatible with oils and do not cause adverse effects on the lubricant. The properties of palm oil are given in Table 1.

2.2. SEM Images. SEM image was used to examine the surface morphology of the nanoparticles. SEM images of the nanoparticles TiO_2 and CuO have been observed and shown in Figure 1. It ensures that the nanoparticles are in the nanometer size range and that the size is marked on the image. Figure 1(a) shows that CuO nanoparticles are in the range of 124 to 215 nm. According to the SEM image, as

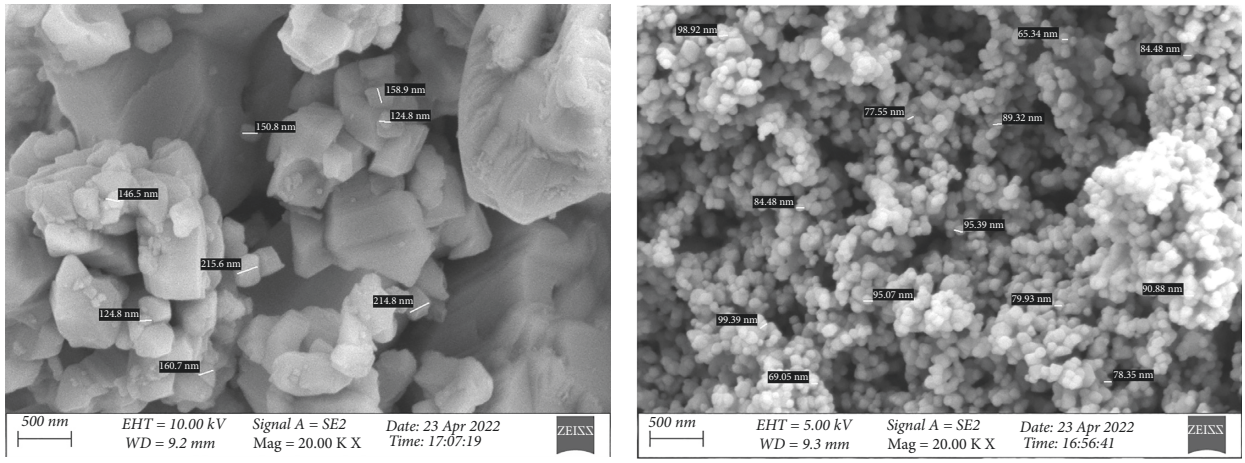

(a) (b)

Figure 1: (a) SEM image of CuO. (b) SEM image of TiO_2.

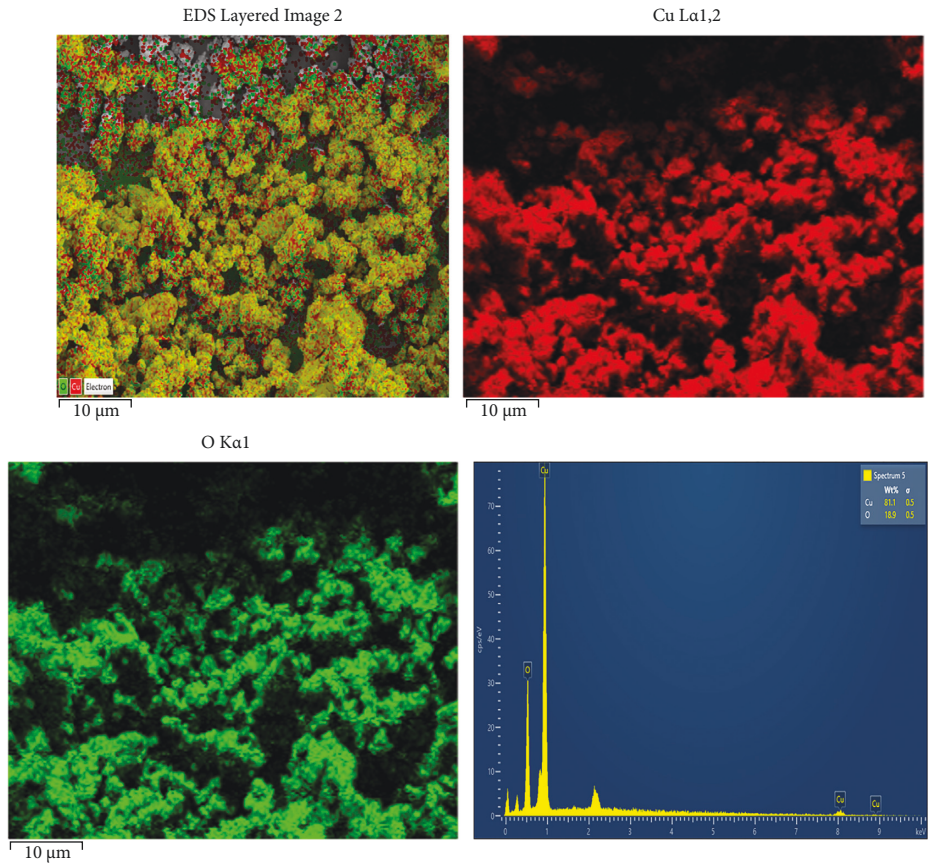

Figure 2: EDX analysis and elemental mapping of CuO.

shown in Figure 1(b), the TiO_2 nanoparticles are 60 to 100 nm in size, and the TiO_2 nanoparticles have a homogeneous spherical morphology.

2.3. EDX of CuO and TiO_2. The energy dispersive X-ray (EDX) analysis is used to characterize the elemental composition and chemical composition of a specimen with an atomic number. Elemental mapping is a technique for obtaining high-resolution imaging by accumulating detailed elemental composition data across a sample area. Every pixel in the image is examined to preserve the rudimentary spectrum.

The EDX spectrum of CuO Nanoparticles is shown in Figure 2. The spectrum depicts the chemical components of the sample. The dissemination of Cu (red dots) and O (green dots) components, which make up the whole body of the

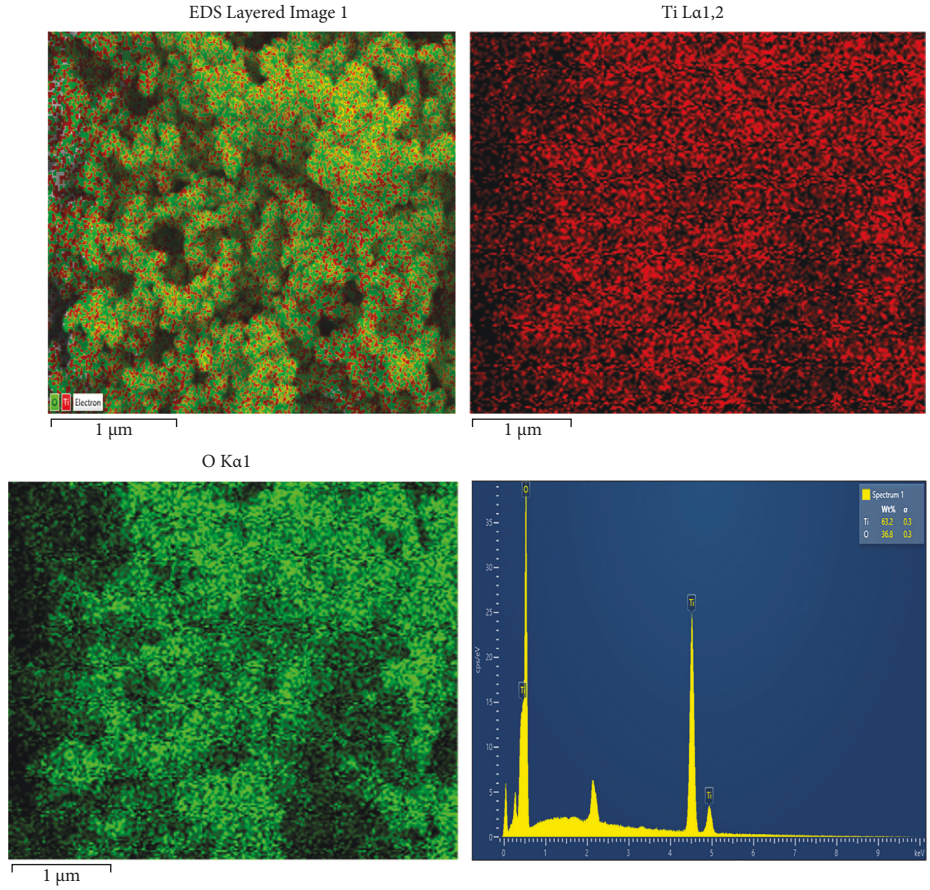

Figure 3: EDX analysis and elemental mapping of TiO_2.

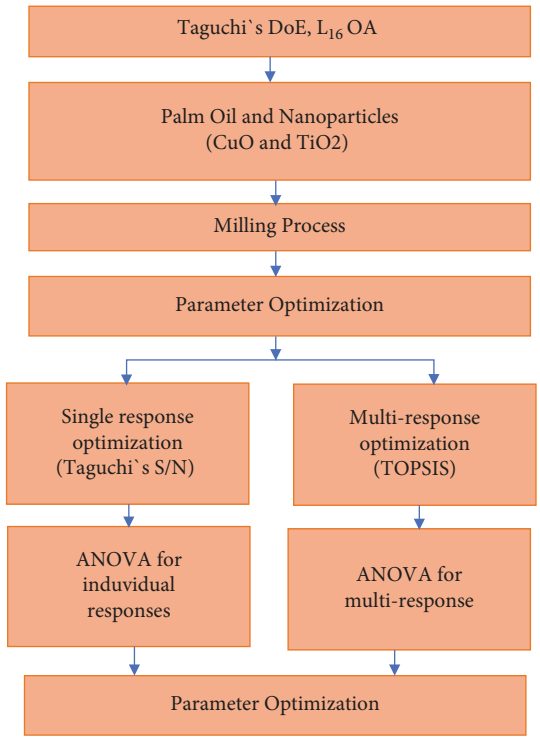

Figure 4: Flowchart for methodology.

processed sample, is homogeneous in Figure 2. For each element, the corresponding findings are shown separately. The presence of oxygen and copper is demonstrated by the change in the distribution of both elements. Figure 2 indicates that 81.1% of Cu and 18.9% of O were presented in the sample. The elemental mapping shows that elements are correctly dispersed in aggregated Cu and O nanoparticles [27]. Figure 2 shows no CuO nanoparticle impurities, and only Cu and O elements are present [28, 29].

Figure 3 shows EDX analysis of TiO_2 nanoparticles. Figure 3 reveals that 63.2% of Ti and 36.8% of O were presented in the sample. The distribution of Ti (red dots) and O (green dots) elements, which make up the entire body of the processed samples, is homogeneous [30, 31]. The results of EDS revealed that no other impurities were present in the nanoparticles. From Figure 3, it was observed that there is no impurity in the TiO_2 nanoparticle, and only the elements Ti and O were present [32, 33].

2.4. Methodology. The flowchart of the methodology for this research is given in Figure 4.

2.4.1. Experimental Setup. Milling operations were completed on a high-rigidity Computer Numerical Control (CNC) BMV35 T12 with a machine with specifications: maximum spindle rpm 8000, spindle power 5.5 kW, and

Table 2: Factors and their levels.

Levels	Spindle speed (rpm)	Feedrate (mm/min)	Depth of cut(mm)	Coolant
Level 1	1500	125	0.10	1 (palm oil)
Level 2	2000	150	0.15	2 (palm oil with 0.5 wt% of CuO)
Level 3	2500	175	0.20	3 (palm oil with 0.5 wt% of TiO_2)
Level 4	3000	200	0.25	4 (palm oil with 0.25 wt% of CuO and 0.25wt% of TiO_2)

Figure 5: (a) 0.5wt% of CuO, (b) 0.5wt% of TiO_2 nanoparticles, (c) hybrid (0.25 wt% of CuO + 0.25wt% of TiO_2).

maximum traverse distance in *x-y-z* axis are 450-350-350 mm, respectively. Commercially available Inconel 625 block (150 × 50 × 50 mm) was used as the workpiece material for machining. End milling operation was selected as the machining process. The cutting tool used for machining Inconel 625 was PVD-coated carbide (Grade: VP15TF; designated as SEMT13T3AGSN-JM).

2.4.2. DoE. Feed rate, spindle speed, cut depth, and palm oil are process parameters. At the same time, the surface roughness, spindle vibration, and material removal rate are considered responses. An orthogonal array (OA) matrix helps the machine operator decide the best parameters with the fewest possible experiments. The four-parameter system has a total of 15 degrees of freedom. An OA's Degree of Freedom (DoF) should be equal to or larger than the total DoF. As a result, L_{16} OA was used in this study because it has a DoF of 15 and allows fewer experiments to identify the best milling parameters. The selected parameters and their levels are shown in Table 2. There are sixteen experiments in total. Experiments are carried out after the OA has been defined, and the S/N for every experiment is calculated [34].

2.4.3. Preparation of Coolant. A beaker of 200 ml was taken, and 99.5 ml of palm oil was poured into it. 0.5 g of nanoparticles was measured using a highly sensitive electronic

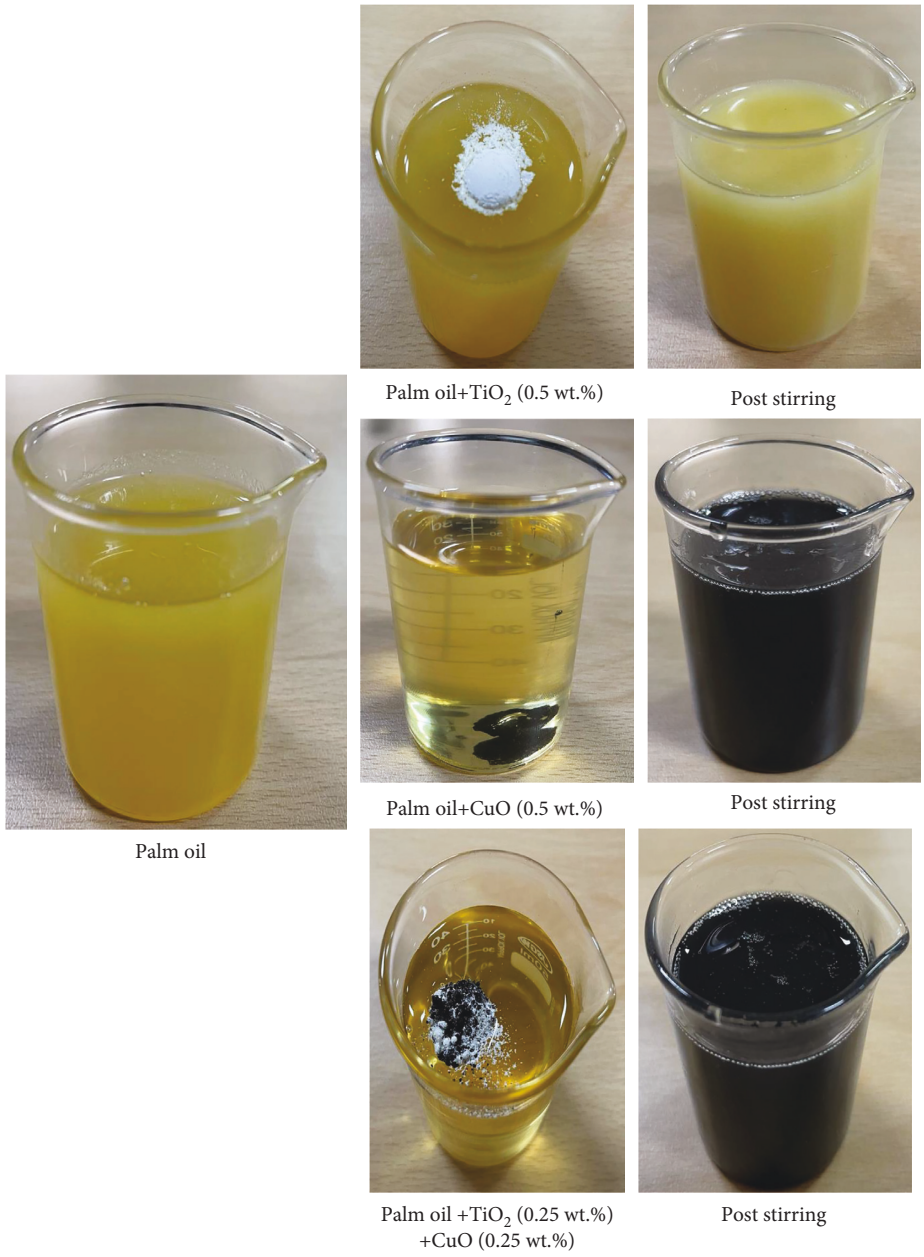

Figure 6: Preparation of nano lubricant.

balance. The electronic balance was air-tight to ensure minimal error. The nanoparticle was poured into the beaker, and constant stirring was done for thirty seconds using a spatula. The stirring ensures that the oil has 0.5 wt% of nanoparticles uniformly [35]. The nanoparticles and preparation of nanolubricant are shown in Figures 5 and 6.

2.4.4. Milling Procedure. The CNC machine BMV35 T12 was used for all milling operations on Inconel 625, as shown in Figure 7. The vibration sensor MPU 6050 has been soldered to the Arduino UNO board using jumper cables. The Arduino UNO board acts as an interface between the sensor and the system and is connected to a laptop using a USB-A cable.

The vibration sensor MPU 6050 has been attached to the spindle using double-sided tape. Using the Arduino IDE, vibration in the spindle's x-, y-, and z-axes during the milling process has been recorded. The workpiece is cleaned with a neat cloth before fitting inside the CNC machine. Facing the workpiece has been done to 0.1 mm. After facing the material, the tool holder is removed and replaced with milling inserts. The mixture of oils and nanoparticles has been poured uniformly over the material using a dropper (10 ml). The end milling operation has been carried out according to the DoE design matrix. After machining, the surface roughness was measured using a surface roughness testing instrument (Make- Carl Zeiss. Model- E-35B). Three surface roughness values were recorded, and the average surface roughness was noted. The material removal rate (MRR) was

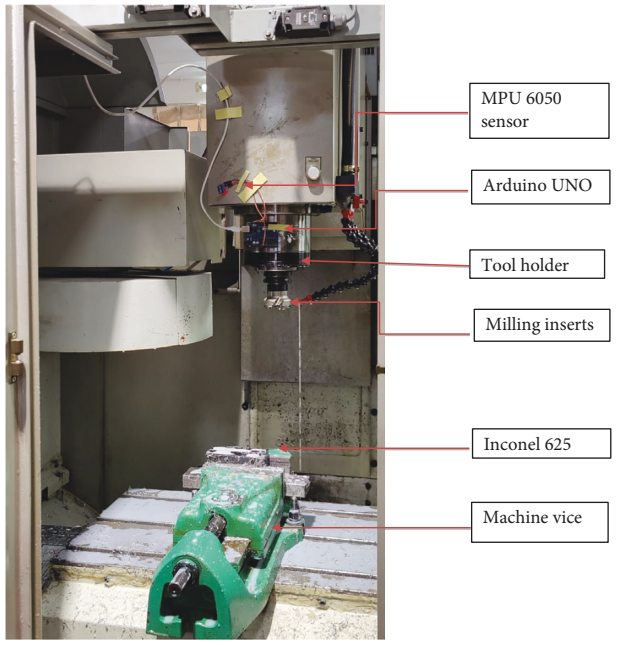

Figure 7: Machining process.

computed using the weight-loss method, and the weight of the material was recorded before and after each pass. The formula for the weight-loss method has been given as follows:

$$\begin{aligned} \text{Loss of material weight}\,(g) &= \textit{original weight} \\ &\quad - \textit{measured weight}, \\ \textit{Volume of workpiece} &= \frac{\text{mass (Loss of material)}}{\text{density}}, \\ \text{MRR} &= \frac{\textit{Volume of workpiece}}{\text{machining time}}. \end{aligned} \tag{1}$$

The density of Inconel 625 is 8.4 g/cc. The same procedure is repeated for all experiments.

2.5. Process Parameter Optimization

2.5.1. Taguchi's S/N. Using Taguchi signal-to-noise (S/N), the optimal factors were analyzed. Larger is better (LB) and Smaller is better (SB) are the two characteristics available for optimization. LR characteristics were applied for MRR and SR characteristics for Ra and *Vx*, *Vy*, and *Vz*. Using the formula, S/N values for different responses were recorded [36–38].

$$\begin{aligned} SB\text{: } \eta &= -10\log\frac{1}{n}\sum_{i=1}^{n} y_i^2, \\ LB &= -10\log\frac{1}{n}\sum_{i=1}^{n} y_i^2. \end{aligned} \tag{2}$$

The S/N ratio was used to determine the best conditions for each response. The ideal situation is the level at which the maximum S/N is reached.

2.6. TOPSIS. To turn a multiresponse optimization problem into a single-response optimization problem, TOPSIS is used. The steps involved in the TOPSIS approach are depicted below. A normalized matrix is utilized in TOPSIS. Calculate the PIS and NIS using normalized weighted values and Euclidean distance using formulae [39, 40]. The S/N for closeness coefficient was computed from that the optimal parameter for multiresponse was identified.

(1) Normalization matrix r_{ij} is calculated out using

$$r_{ij} = \frac{x_{ij}}{\sqrt{\sum_{i=1}^{m} x_{ij}^2}}, \tag{3}$$

where $i = 1, 2, 3, \ldots, m$, $j = 1, 2, 3, \ldots, n$ and a_{ij} represent the i^{th} value of the j^{th} experimental run. r_{ij} represents the normalized data for the corresponding test.

(2) Compute the weight w_{ij} of each response.

(3) The weighted normalized data is computed by multiplying the normalized data with its equivalent weight. The weighted normalized data V_{ij} is computed using

$$V_{ij} = w_i * r_{ij}, \tag{4}$$

where $i = 1, 2, \ldots, m$, $j = 1, 2, \ldots, n$ and w_j represents the weight of the j^{th} criterion

$$\sum_{j=1}^{n} \mathrm{w_j} = 1. \tag{5}$$

(4) The PIS (V^+) and NIS (V^-) are estimated from the weighted normalized data:

$$V^+ = (V_1^+, V_2^+, \ldots, V_n^+)\max \textit{values}, \tag{6}$$

$$V^- = (V_1^-, V_2^-, \ldots, V_n^-)\max \textit{values}. \tag{7}$$

(5) The separation value of the PIS and NIS is computed from (6) and (7):

$$\begin{aligned} S_i^+ &= \sqrt{\sum_{j=1}^{n} \left(V_{ij} - V_j^+\right)^2}, \\ S_i^- &= \sqrt{\sum_{j=1}^{n} \left(V_{ij} - V_j^-\right)^2}, \end{aligned} \tag{8}$$

where $i = 1, 2, \ldots, m$.

(6) The closeness coefficient to the ideal solution is estimated using equation (11):

Table 3: Surface roughness, spindle vibration, and MRR for palm oil.

Speed	Feed	DoC	Coolant	Ra	MRR	ax	ay	az
1500	125	0.1	1	0.103	1.191198	0.173359	0.417925	0.396441
1500	150	0.15	2	0.149	1.435532	0.166886	0.406583	0.358339
1500	175	0.2	3	0.159	3.361345	0.176182	0.442583	0.396144
1500	200	0.25	4	0.229	3.494976	0.213174	0.406836	0.375259
2000	125	0.15	3	0.076	2.021427	0.164513	0.422058	0.393962
2000	150	0.1	4	0.163	2.436054	0.178955	0.414779	0.391988
2000	175	0.25	1	0.161	7.510504	0.114595	0.42088	0.377286
2000	200	0.2	2	0.35	7.809087	0.180548	0.435534	0.406443
2500	125	0.2	4	0.103	1.155101	0.220654	0.432775	0.409345
2500	150	0.25	3	0.081	1.392031	0.200459	0.429581	0.381369
2500	175	0.1	2	0.12	3.571429	0.166229	0.425354	0.386759
2500	200	0.15	1	0.111	3.713412	0.184046	0.427508	0.39247
3000	125	0.25	2	0.108	1.010714	0.179596	0.416428	0.36319
3000	150	0.2	1	0.11	1.218027	0.178492	0.43709	0.393807
3000	175	0.15	4	0.07	2.258403	0.148024	0.422805	0.367047
3000	200	0.1	3	0.107	2.348187	0.191256	0.437669	0.384296

Table 4: S/N values for individual responses.

	Level	Speed	Feed	DoC	Coolant
Smaller is better					
Ra	1	16.26	20.3	18.33	18.47
	2	15.78	18.32	20.28	15.85
	3	19.77	18.34	16	19.9
	4	20.25	15.11	17.46	17.85
	Delta	4.47	5.19	4.28	4.05
	Rank	2	1	3	4
Vx	1	14.82	14.73	15.03	15.93
	2	16.08	14.86	15.63	15.23
	3	14.34	16.52	14.51	14.77
	4	15.21	14.34	15.28	14.52
	Delta	1.73	2.18	1.12	1.4
	Rank	2	1	4	3
Vy	1	7.572	7.489	7.456	7.416
	2	7.468	7.497	7.542	7.518
	3	7.355	7.375	7.191	7.272
	4	7.363	7.397	7.569	7.552
	Delta	0.217	0.122	0.378	0.28
	Rank	3	4	1	2
Vz	1	8.376	8.16	8.182	8.193
	2	8.146	8.42	8.448	8.446
	3	8.184	8.396	7.912	8.25
	4	8.459	8.19	8.623	8.277
	Delta	0.314	0.261	0.711	0.253
	Rank	2	3	1	4
Larger is better					
MRR	1	6.515	2.244	6.931	8.035
	2	12.303	3.865	6.931	8.020
	3	6.644	11.544	7.837	6.733
	4	4.074	11.883	7.834	6.733
	Delta	8.229	9.638	0.906	1.303
	Rank	2	1	4	3

Table 5: Analysis of variance.

Source	DF	Adj SS	Adj MS	F-Value	*P*-Value	% Contribution
Surface roughness						
Speed	3	0.02259	0.007529	21.92	0.015	31.02
Feed	3	0.02261	0.007535	21.94	0.015	31.04
DoC	3	0.0136	0.004534	13.2	0.031	18.68
Coolant	3	0.01298	0.004326	12.59	0.033	17.82
Error	3	0.00103	0.000344			
Total	15	0.0728				
S		R-sq		R-sq(adj)		R-sq(pred)
0.018534		98.58%		92.92%		89.74%
MRR						
Speed	3	24.28	8.0932	21.08	0.016	37.06
Feed	3	31.03	10.3433	26.94	0.011	47.36
DoC	3	3.98	1.3267	3.46	0.168	6.07
Coolant	3	5.065	1.6883	4.4	0.128	7.73
Error	3	1.152	0.384			
Total	15	65.506				
S		R-sq		R-sq(adj)		R-sq(pred)
0.61964		98.24%		91.21%		49.98%
Vx						
Speed	3	0.00235	0.000784	16.72	0.022	25.66
Feed	3	0.00388	0.001292	27.57	0.011	42.31
DoC	3	0.00107	0.000356	7.6	0.065	11.65
Coolant	3	0.00173	0.000575	12.27	0.034	18.83
Error	3	0.00014	0.000047			
Total	15	0.00916				
S		R-sq		R-sq(adj)		R-sq(pred)
0.006846		98.47%		92.33%		86.35%
Vy						
Speed	3	0.00029	0.000096	10.26	0.044	16.48
Feed	3	0.00011	0.000037	4.01	0.142	6.43
DoC	3	0.00086	0.000288	30.81	0.009	49.56
Coolant	3	0.00045	0.00015	16.12	0.024	25.90
Error	3	2.8E-05	0.000009			
Total	15	0.00174				
S		R-sq		R-sq(adj)		R-sq(pred)
0.0030549		98.39%		91.96%		84.27%
Vz						
Speed	3	0.00073	0.000243	9.64	0.048	22.54
Feed	3	0.0003	0.000099	3.93	0.145	9.20
DoC	3	0.00182	0.000607	24.04	0.013	56.23
Coolant	3	0.00031	0.000104	4.13	0.137	9.66
Error	3	7.6E-05	0.000025			
Total	15	0.00324				
S		R-sq		R-sq(adj)		R-sq(pred)
0.0063477		96.66%		85.31%		83.06%

$$CC_i^+ = \frac{S_i^-}{S_i^+ + S_i^-}. \quad (9)$$

3. Results and Discussion

3.1. Single Response Optimization Using Taguchi's S/N. The surface roughness, MRR, and spindle vibrations are tabulated in Table 3.

Taguchi's S/N values were used to find the best parameters for individual responses. The SB characteristics were used for surface roughness and vibration signals. Maximizing the MRR is a critical criterion in metal removal processes [41]. The MRR must be determined to attain excellent machinability. As a result, for MRR, the LB characteristic was used. From Table 4, it can be seen that the highest S/N value produces the best results. For palm oil, the minimum surface roughness can be obtained when the spindle speed is 3000 rpm, feed rate of 125 mm/min, depth of cut (DoC) of 0.15 mm, and palm oil, with CuO nanoparticles being used as a coolant. Minimal vibration on the *x*-axis during the machining operation was obtained with the spindle speed of 2000 rpm, feed rate of 175 mm/min, DoC of 0.15 mm, and palm oil without nanoparticles. Similarly, for the *y*-axis and *z*-axis speeds of 1500 rpm and 3000 rpm, a feed rate of 150 mm/min for both DoC of 0.25 mm for both

and y-axis palm oil with both nanoparticles and z-axis palm oil, with TiO_2 being used as the coolant. For MRR, the optimal parameters are a speed of 2000 rpm, 200 mm/min feed, 0.20 mm DoC, and palm oil without nanoparticles.

3.2. ANOVA. Analysis of Variance (ANOVA) is used to find the most significant parameter influencing the response. When using ANOVA, the method is quite beneficial for determining the level of risk and the effect of milling parameters on a specific response. It is utilized to determine each control factor's relative influence in the response evaluation to ensure that the quality of the most critical aspects of the product should be carefully monitored [22, 42].

3.2.1. Surface Roughness. From Table 5, both speed and feed rate have the same level of contribution of 31% to surface roughness, followed by DoC of 18.68% and coolant of 17.82%, respectively. From the P-value ($P < 0.05$), it was found that all parameters have significantly impacted machining. The average surface roughness for the speed of 1500 rpm is 0.16 μm, and when the speed increases to 2500 rpm, the surface roughness is reduced by 18.75%. Similarly, for the speed of 3000 rpm, there is a 38.75% decrease in surface roughness. As the spindle speed increases, the built-up edge advancement slows down, and heat in the shear zone rises, making it more straightforward for machining and improving surface quality [43]. With an increase in feed, the surface roughness steadily increased, generating force on the machined surface that causes vibration, which raises the roughness. An identical pattern was observed in the literature [21, 44].

It is observed that when CuO and TiO_2 (hybrid mode) nanoparticles are mixed with palm oil, the lowest surface roughness is obtained when compared to all other combinations [45]. The mechanism could involve rolling CuO nanoparticles rather than forming a layer or repairing surfaces [46]. CuO nanoparticles act as a third body between the two mating parts, preventing metal-metal contact and thus reducing surface roughness, as evidenced by the lower coefficient of friction and roughness values observed [47].

3.2.2. MRR. From Table 5, it was observed that feed has a significant impact on the MRR, contributing 47.36%. Moreover, the speed gives 37.06% of the contribution to the machining process. DoC and coolant have an insignificant impact of 6.07% and 7.73%. The feed has more impact than speed and as the feed increases, machining the material to the desired length takes less time, increasing the MRR [48]. When palm oil is mixed with the hybrid combination of nanoparticles at a speed of 2000 rpm, a feed of 175 mm/min, and 0.15 mm DoC, the optimal results are obtained. The hybrid mode of nanoparticles formulates a third layer between the workpiece and the tool. The surface is slippery, will be long-lasting, and is ideal for machining for extended periods [49].

Table 6: Normalization table.

S. No.	Ra	MRR	V_x	V_y	V_z
1	0.168131	0.084796	0.242232	0.245895	0.256665
2	0.243218	0.102189	0.233188	0.239221	0.231997
3	0.259541	0.23928	0.246177	0.260403	0.256473
4	0.373805	0.248793	0.297865	0.23937	0.242951
5	0.124058	0.143897	0.229872	0.248327	0.25506
6	0.266071	0.173412	0.250051	0.244044	0.253782
7	0.262806	0.534641	0.160123	0.247633	0.244264
8	0.571318	0.555896	0.252278	0.256255	0.26314
9	0.168131	0.082227	0.308317	0.254632	0.26502
10	0.132219	0.099093	0.280098	0.252753	0.246907
11	0.19588	0.254235	0.232269	0.250266	0.250397
12	0.181189	0.264342	0.257165	0.251533	0.254094
13	0.176292	0.071948	0.250947	0.245014	0.235137
14	0.179557	0.086706	0.249405	0.257171	0.25496
15	0.114264	0.160766	0.206832	0.248766	0.237635
16	0.17466	0.167158	0.267239	0.257512	0.248802

3.2.3. Spindle Vibration. From Table 5, it can see that x-axis feed can have a significant impact of 42.31%, followed by a speed of 25.66%, and coolant of 18.83%. DoC also has a minimal impact of 11.65%. All parameters will have a significant impact on the machining process. For the y-axis, the DoC had a significant contribution of 49.56%, followed by coolant with 25.9% and speed with 16.48%, and feed had an insignificant impact of 6.43% [50]. For the z-axis, DoC had a significant impact of 56.23%, followed by a speed of 22.54%, and both the coolant and depth of cut had an insignificant impact of 9.6% and 9.2%, respectively. The spindle moves in the same direction as the z-axis. As a result, the contribution of the DoC is more on the z-axis [34, 51].

It is observed that when using vibration on the x-axis, the values are lower when TiO_2 is mixed with palm oil [52]. Similarly, for the z-axis, the values are lower when TiO_2 is mixed with palm oil [53]. Similar research discovered that adding nanoparticles to the lubricant can decrease friction and wear, increase allowable bearing capacity, and remove heat under higher temperatures and high load conditions, reducing bearing wear and achieving vibration suppression [54].

4. Multiresponse Optimization Using TOPSIS

TOPSIS can be used to conduct multiresponse optimization. Table 6 displays the normalized data. (3) can be used to conduct data normalization. Table 7 shows the weighted normalization and separation measures. (4) is used to calculate the weighted normalization. Equations (8), (9), and (11) calculate the separation measures and the closeness coefficient CC_i. Table 8 shows the S/N values of CC_i. From Table 8, it can see that the optimal parameter can be identified. The optimal parameters are the speed of 2000 rpm, feed of 175 mm/min feed, DoC of 0.15 mm, and palm oil with 0.25 wt% of CuO and 0.25wt% of TiO_2 nanoparticles. From Table 9, it can be seen that the feed had a contribution of 43.93%, followed by a speed of 25.10%, the coolant of 23.3%, and DoC of 6.08%. Speed, feed, and coolant significantly impacted the machining process. From this, it can be observed that the multiresponse characteristics are impacted by feed speed and coolant.

Table 7: Weighted normalization. Measures of separation and closeness coefficient values.

Ra	MRR	V_x	V_y	V_z	S^+	S^-	CC_i
0.033626	0.016959	0.048446	0.049179	0.051333	0.096381	0.081822	0.459152
0.048644	0.020438	0.046638	0.047844	0.046399	0.09546	0.068043	0.416158
0.051908	0.047856	0.049235	0.052081	0.051295	0.072057	0.071872	0.499357
0.074761	0.049759	0.059573	0.047874	0.04859	0.085033	0.053413	0.385803
0.024812	0.028779	0.045974	0.049665	0.051012	0.083742	0.092004	0.523504
0.053214	0.034682	0.05001	0.048809	0.050756	0.084362	0.065501	0.437072
0.052561	0.106928	0.032025	0.049527	0.048853	0.030158	0.115207	0.792536
0.114264	0.111179	0.050456	0.051251	0.052628	0.09352	0.097441	0.510264
0.033626	0.016445	0.061663	0.050926	0.053004	0.100111	0.080672	0.446237
0.026444	0.019819	0.05602	0.050551	0.049381	0.094613	0.088256	0.482618
0.039176	0.050847	0.046454	0.050053	0.050079	0.064289	0.084919	0.569133
0.036238	0.052868	0.051433	0.050307	0.050819	0.0631	0.087642	0.581406
0.035258	0.01439	0.050189	0.049003	0.047027	0.099266	0.080116	0.446623
0.035911	0.017341	0.049881	0.051434	0.050992	0.096586	0.079316	0.45091
0.022853	0.032153	0.041366	0.049753	0.047527	0.079607	0.095493	0.545362
0.034932	0.033432	0.053448	0.051502	0.04976	0.081696	0.082064	0.501122

Table 8: S/N for TOPSIS.

Level	Speed	Feed	DoC	Coolant
1	−7.17	−6.749	−6.392	−5.215
2	−5.281	−7.012	−5.803	−6.339
3	−5.887	−4.666	−6.602	−6.176
4	−6.477	−6.388	−6.018	−5.085
Delta	1.889	2.347	0.799	1.871
Rank	2	1	4	3

Table 9: ANOVA for CC_i.

Source	DF	Adj SS	Adj MS	F-value	*P*-value	% contribution
Speed	3	0.02949	0.009828	15.94	0.024	25.10
Feed	3	0.05159	0.017197	27.89	0.011	43.93
DoC	3	0.00715	0.002382	3.86	0.148	6.08
Coolant	3	0.02737	0.009122	14.8	0.027	23.30
Error	3	0.00185	0.000617			
Total	15	0.11744				

Table 10: Confirmation test results.

Responses	Optimal parameters	Measured values	TOPSIS	Measured values	Variation	% improvement
Ra	A4-B1-C2- D3	0.170975		0.16567	0.00530	3.10
MRR	A2-B4-C3-D1	3.58		3.80	0.22	6.14
V_x	A2-B3-C2-D1	0.176825	A2-B3-C2-D4	0.16348	0.0133	7.54
V_y	A1-B2-C4-D4	0.42075		0.44364	−0.02289	−5.44
V_z	A4-B2-C4-D2	0.38335		0.35735	0.026	6.78

4.1. Confirmation Test. A calculation test was used to verify the significance of the solution parameters. The experiments were repeated three times, with the average result used for the analysis. For further investigation, the value was used. Table 10 showed the confirmation test results and discovered that the surface roughness decreased by 3.10%. The MRR was increased by 6.14%. The spindle vibration in the x & z-axis decreased by 7.54% and 6.78%. On the other hand, vibration in the y-axis increased by 5.44%.

The consumption of nanoparticles (0.25 to 0.5 wt%) along with palm oil is significantly less, and the overall cost is also reasonably minimum. Further, it enhances the surface roughness, MRR, and vibration features. This will significantly enhance the life span of the machine.

5. Conclusion

Inconel 625 was machined with SEMT-13T3AGSN-JM VP15 TF with palm oil and CuO and TiO_2 nanoparticles as additives. Taguchi's DoE was applied to design the experiments. Taguchi's DoE coupled with TOPSIS was used to optimize the process parameters. The following conclusions have been drawn from the experimentation:

(i) Surface roughness was measured as a feed and speed function and depended on it.

(ii) Both the speed and feed significantly impact MRR.

(iii) The spindle speed vibration in the x-axis depends on the speed and feed. Similarly, the y-axis depends on the DoC and coolant, and the z-axis depends on the depth of cut and speed.

(iv) Taguchi's S/N analysis was used to find the best parameters for individual responses.

(v) TOPSIS was used to perform the multiresponse optimization, with the best parameters being 2000 rpm, 175 mm/min feed, 0.15 mm depth, and coolant of palm oil with 0.25 wt% of CuO and 0.25wt% of TiO_2 nanoparticles.

(vi) According to ANOVA for the closeness coefficient, speed and feed have physical significance, with 25.10% and 43.93%, respectively.

(vii) Surface roughness, material removal rate, and spindle speed vibration were reduced by 3.10%, 6.14 percent, 7.54% (Vx), and 6.78%(Vz) due to TOPSIS optimization. This will significantly improve the machining performance.

Data Availability

The data used to support the findings of this study are included within the article.

Conflicts of Interest

The authors declare that they have no conflicts of interest.

References

[1] O. Çolak, "Investigation on machining performance of inconel 718 under high pressure cooling conditions," *Strojniški vestnik-Journal of Mechanical Engineering*, vol. 58, no. 11, pp. 683–690, 2012.

[2] J. S. Senthilkumaar, P. Selvarani, and R. M. Arunachalam, "Intelligent optimization and selection of machining parameters in finish turning and facing of Inconel 718," *International Journal of Advanced Manufacturing Technology*, vol. 58, no. 9-12, pp. 885–894, 2012.

[3] D. G. Thakur, B. Ramamoorthy, and L. Vijayaraghavan, "Investigation and optimization of lubrication parameters in high speed turning of superalloy Inconel 718," *International Journal of Advanced Manufacturing Technology*, vol. 50, no. 5-8, pp. 471–478, 2010.

[4] N. Dhar, M. Kamruzzaman, and M. Ahmed, "Effect of minimum quantity lubrication (MQL) on tool wear and surface roughness in turning AISI-4340 steel," *Journal of Materials Processing Technology*, vol. 172, no. 2, pp. 299–304, 2006.

[5] A. K. Sharma, A. K. Tiwari, and A. R. Dixit, "Effects of Minimum Quantity Lubrication (MQL) in machining processes using conventional and nanofluid based cutting fluids: a comprehensive review," *Journal of Cleaner Production*, vol. 127, pp. 1–18, 2016.

[6] T. Singh, P. Singh, J. Dureja, M. Dogra, H. Singh, and M. S. Bhatti, "A review of near dry machining/minimum quantity lubrication machining of difficult to machine alloys," *International Journal of Machining and Machinability of Materials*, vol. 18, no. 3, pp. 213–251, 2016.

[7] J. P. Davim, P. S. Sreejith, and J. Silva, "Turning of brasses using minimum quantity of lubricant (MQL) and flooded lubricant conditions," *Materials and Manufacturing Processes*, vol. 22, no. 1, pp. 45–50, 2007.

[8] N. Radhika, A. Sudhamshu, and G. K. Chandran, "Optimization of electrical discharge machining parameters of aluminium hybrid composites using Taguchi method," *Journal of Engineering Science & Technology*, vol. 9, no. 4, pp. 502–512, 2014.

[9] A. Devillez, G. Le Coz, S. Dominiak, and D. Dudzinski, "Dry machining of Inconel 718, workpiece surface integrity," *Journal of Materials Processing Technology*, vol. 211, no. 10, pp. 1590–1598, 2011.

[10] H. Kumar, S. Ilangovan, and N. Radhika, "Optimization of cutting parameters for MRR, tool wear and surface roughness characteristics in machining ADC12 piston alloy using DOE," *Tribology in industry*, vol. 42, no. 1, pp. 32–40, 2020.

[11] D. Thakur, B. Ramamoorthy, and L. Vijayaraghavan, "Influence of minimum quantity lubrication on the high speed turning of aerospace material superalloy Inconel 718," *International Journal of Machining and Machinability of Materials*, vol. 13, no. 2/3, pp. 203–214, 2013.

[12] I. Choudhury and M. El-Baradie, "Machinability of nickel-base super alloys: a general review," *Journal of Materials Processing Technology*, vol. 77, no. 1–3, pp. 278–284, 1998.

[13] M. Mia, M. K. Gupta, J. A. Lozano et al., "Multi-objective optimization and life cycle assessment of eco-friendly cryogenic N2 assisted turning of Ti-6Al-4V," *Journal of Cleaner Production*, vol. 210, pp. 121–133, 2019.

[14] M. K. Gupta, M. Mia, G. Singh, D. Y. Pimenov, M. Sarikaya, and V. S. Sharma, "Hybrid cooling-lubrication strategies to improve surface topography and tool wear in sustainable turning of Al 7075-T6 alloy," *International Journal of Advanced Manufacturing Technology*, vol. 101, no. 1–4, pp. 55–69, 2019.

[15] M. Sarıkaya, V. Yılmaz, and A. Güllü, "Analysis of cutting parameters and cooling/lubrication methods for sustainable machining in turning of Haynes 25 superalloy," *Journal of Cleaner Production*, vol. 133, pp. 172–181, 2016.

[16] Ç V. Yıldırım, T. Kivak, M. Sarikaya, and F. Erzincanli, "Determination of MQL parameters contributing to sustainable machining in the milling of nickel-base superalloy waspaloy," *Arabian Journal for Science and Engineering*, vol. 42, no. 11, pp. 4667–4681, 2017.

[17] Y. Su, L. Gong, B. Li, Z. Liu, and D. Chen, "Performance evaluation of nanofluid MQL with vegetable-based oil and ester oil as base fluids in turning," *International Journal of Advanced Manufacturing Technology*, vol. 83, no. 9–12, pp. 2083–2089, 2016.

[18] N. C. Sidik and O. A. Alawi, "Computational investigations on heat transfer enhancement using nanorefrigerants," *Journal of Advanced Research Design*, vol. 1, pp. 35–41, 2014.

[19] M. Jamil, N. C. Sidik, and M. M. Yazid, "Thermal performance of thermosyphon evacuated tube solar collector using TiO2/water nanofluid," *Journal of Advanced Research in Fluid Mechanics and Thermal Sciences*, vol. 20, no. 1, pp. 12–29, 2016.

[20] S. Zainal, "ANSYS simulation for Ag/HEG hybrid nanofluid in turbulent circular pipe," *Journal of Advanced Research in Applied Mechanics*, vol. 23, no. 1, pp. 20–35, 2016.

[21] S. R. Das, D. Dhupal, and A. Kumar, "Experimental investigation into machinability of hardened AISI 4140 steel using TiN coated ceramic tool," *Measurement*, vol. 62, pp. 108–126, 2015.

[22] A. C. Mitra, M. Jawarkar, T. Soni, and G. Kiranchand, "Implementation of Taguchi method for robust suspension design," *Procedia Engineering*, vol. 144, pp. 77–84, 2016.

[23] V. Vignesh, S. Ilangovan, and N. Radhika, "Statistical analysis of process parameters in drilling of SS410 stainless steel," *Materials Today Proceedings*, vol. 46, pp. 3313–3319, 2021.

[24] H.-S. Shih, H.-J. Shyur, and E. S. Lee, "An extension of TOPSIS for group decision making," *Mathematical and Computer Modelling*, vol. 45, no. 7-8, pp. 801–813, 2007.

[25] S. V. Alagarsamy, P. Raveendran, and M. Ravichandran, "Investigation of material removal rate and tool wear rate in spark erosion machining of Al-Fe-Si alloy composite using taguchi coupled TOPSIS approach," *Silicon*, vol. 13, no. 8, pp. 2529–2543, 2021.

[26] M. Thangamuthu, J. Yerchuru, N. A. R. Shanmugam, Y. Ravi, and A. K. Gur, "Multi-response optimization of end-milling parameters for inconel 625 using taguchi coupled with topsis," *Surface Review and Letters*, vol. 28, no. 10, Article ID 2150096, 2021.

[27] S. I. Al-Saeedi, G. M. Al-Senani, O. H. Abd-Elkader, and N. M. Deraz, "One pot synthesis, surface and magnetic properties of Cu2O/Cu and Cu2O/CuO nanocomposites," *Crystals*, vol. 11, no. 7, p. 751, 2021.

[28] M. Verma, V. Kumar, and A. Katoch, "Sputtering based synthesis of CuO nanoparticles and their structural, thermal and optical studies," *Materials Science in Semiconductor Processing*, vol. 76, pp. 55–60, 2018.

[29] D. Rehana, D. Mahendiran, R. S. Kumar, and A. K. Rahiman, "Evaluation of antioxidant and anticancer activity of copper oxide nanoparticles synthesized using medicinally important plant extracts," *Biomedicine & Pharmacotherapy*, vol. 89, pp. 1067–1077, 2017.

[30] A. M. Alturki and R. Ayad, "Synthesis and characterization of titanium dioxide nanoparticles with a dosimetry study of their ability to enhance radiation therapy using a low energy X-ray source," *Indian Journal of Science and Technology*, vol. 12, pp. 1–5, 2019.

[31] D. Cabaleiro, M. J. Pastoriza-Gallego, C. Gracia-Fernandez, M. M. Pineiro, and L. Lugo, "Rheological and volumetric properties of TiO2-ethylene glycol nanofluids," *Nanoscale Research Letters*, vol. 8, no. 1, pp. 1–3, 2013.

[32] M. Hamadanian, A. Reisi-Vanani, and A. Majedi, "Sol-gel preparation and characterization of Co/TiO2 nanoparticles: application to the degradation of methyl orange," *Journal of the Iranian Chemical Society*, vol. 7, no. S2, pp. S52–S58, 2010.

[33] M. B. Askari, Z. Tavakoli Banizi, M. Seifi, S. Bagheri Dehaghi, and P. Veisi, "Synthesis of TiO2 nanoparticles and decorated multi-wall carbon nanotube (MWCNT) with anatase TiO2 nanoparticles and study of optical properties and structural characterization of TiO2/MWCNT nanocomposite," *Optik*, vol. 149, pp. 447–454, 2017.

[34] S. Shankar, T. Mohanraj, and A. Pramanik, "Tool condition monitoring while using vegetable based cutting fluids during milling of inconel 625," *Journal of Advanced Manufacturing Systems*, vol. 18, no. 04, pp. 563–581, 2019.

[35] A. Das, O. Pradhan, S. K. Patel, S. R. Das, and B. B. Biswal, "Performance appraisal of various nanofluids during hard machining of AISI 4340 steel," *Journal of Manufacturing Processes*, vol. 46, pp. 248–270, 2019.

[36] J. Gokulachandran and K. Mohandas, "Prediction of cutting tool life based on Taguchi approach with fuzzy logic and support vector regression techniques," *International Journal of Quality & Reliability Management*, vol. 32, no. 3, pp. 270–290, 2015.

[37] A. S. Kang, G. S. Cheema, and V. Gandhi, "Optimization of surface roughness and metal removal rate in end milling using taguchi grey relational analysis," *Indian Journal of Science and Technology*, vol. 10, pp. 31–13, 2017.

[38] A. K. Gur, C.n. Ozay, and B. Icen, "Evaluation of B4c/Ti coating layer, investigation of abrasive wear behaviors using Taguchi technique and response surface methodology," *Surface Review and Letters*, vol. 27, no. 10, Article ID 1950225, 2020.

[39] H.-P. Nguyen, V.-D. Pham, and N.-V. Ngo, "Application of TOPSIS to Taguchi method for multi-characteristic optimization of electrical discharge machining with titanium powder mixed into dielectric fluid," *International Journal of Advanced Manufacturing Technology*, vol. 98, no. 5–8, pp. 1179–1198, 2018.

[40] A. Shanmugam, T. Mohanraj, K. Krishnamurthy, and A. K. Gur, "Multi-response optimization on abrasive waterjet machining of glass fiber reinforced plastics using taguchi method coupled with topsis," *Surface Review and Letters*, vol. 28, no. 12, Article ID 2150120, 2021.

[41] S. Shankar, T. Mohanraj, and S. K. Thangarasu, "Multi-response milling process optimization using the Taguchi method coupled to grey relational analysis," *Materials Testing*, vol. 58, no. 5, pp. 462–470, 2016.

[42] A. K. Gür, T. Yildiz, and B. Icen, "Theoretical evaluation of abrasive wear behavior of B4C/FeCrC coating layer evaluated by a Taguchi approach," *Materials Testing*, vol. 62, no. 7, pp. 733–738, 2020.

[43] M. Yasir, "Effect of cutting speed and feed rate on surface roughness of AISI 316l SS using end-milling," *ARPN Journal of Engineering and Applied Sciences*, vol. 11, no. 4, pp. 2496–2500, 2016.

[44] M. D. Morehead, Y. Huang, and J. Luo, "Chip morphology characterization and modeling in machining hardened 52100 steels," *Machining Science and Technology*, vol. 11, no. 3, pp. 335–354, 2007.

[45] A. Raina and A. Anand, "Influence of surface roughness and nanoparticles concentration on the friction and wear characteristics of PAO base oil," *Materials Research Express*, vol. 5, no. 9, Article ID 095018, 2018.

[46] S. Bhaumik and S. Pathak, "Analysis of anti-wear properties of CuO nanoparticles as friction modifiers in mineral oil (460cSt viscosity) using pin-on-disk tribometer," *Tribology in industry*, vol. 37, no. 2, p. 196, 2015.

[47] M. V. Thottackkad, R. K. Perikinalil, and P. N. Kumarapillai, "Experimental evaluation on the tribological properties of coconut oil by the addition of CuO nanoparticles," *International Journal of Precision Engineering and Manufacturing*, vol. 13, no. 1, pp. 111–116, 2012.

[48] S. Singhvi and M. Khidiya, "Effect of spindle speed and feed on material removal rate in turning operation," *Int. J. Sci. Res. Sci. Eng. Technol*, vol. 2, pp. 807–811, 2016.

[49] I. P. Okokpujie, O. S. Ohunakin, and C. A. Bolu, "Multi-objective optimization of machining factors on surface roughness, material removal rate and cutting force on end-milling using MWCNTs nano-lubricant," *Progress in Additive Manufacturing*, vol. 6, no. 1, pp. 155–178, 2021.

[50] T. Mohanraj, S. Shankar, R. Rajasekar, R. Deivasigamani, and P. M. Arunkumar, "Tool condition monitoring in the milling process with vegetable based cutting fluids using vibration signatures," *Materials Testing*, vol. 61, no. 3, pp. 282–288, 2019.

[51] T. Mohanraj, J. Yerchuru, H. Krishnan, R. Nithin Aravind, and R. Yameni, "Development of tool condition monitoring system in end milling process using wavelet features and Hoelder's exponent with machine learning algorithms," *Measurement*, vol. 173, Article ID 108671, 2021.

[52] S. Singh, X. Chen, C. Zhang, R. K. Gautam, R. Tyagi, and J. Luo, "Nickel-catalyzed direct growth of graphene on bearing steel (GCr15) by thermal chemical vapor deposition and its tribological behavior," *Applied Surface Science*, vol. 502, Article ID 144135, 2020.

[53] V. Bhardwaj, R. Pandey, and V. Agarwal, "Experimental investigations for tribo-dynamic behaviours of conventional and textured races ball bearings using fresh and MoS2 blended greases," *Tribology International*, vol. 113, pp. 149–168, 2017.

[54] D. Muller, C. Matta, R. Thijssen, M. bin Yusof, M. van Eijk, and S. Chatra, "Novel polymer grease microstructure and its proposed lubrication mechanism in rolling/sliding contacts," *Tribology International*, vol. 110, pp. 278–290, 2017.